HHS Public Access

Author manuscript

Pediatr Blood Cancer. Author manuscript; available in PMC 2016 May 10.

Published in final edited form as:

Pediatr Blood Cancer. 2016 February ; 63(2): 206–213. doi:10.1002/pbc.25763.

Preclinical Evidence for the Use of Sunitinib Malate in the Treatment of Plexiform Neurofibromas

Michael J. Ferguson[1,*], **Steven D. Rhodes**[1,2], **Li Jiang**[1,2], **Xiaohong Li**[1,2], **Jin Yuan**[1,2], **Xianlin Yang**[1,2], **Shaobo Zhang**[3], **Saeed T. Vakili**[3], **Paul Territo**[4], **Gary Hutchins**[4], **Feng-Chun Yang**[1,2,5], **David A. Ingram**[1,2], **D. Wade Clapp**[1,2,6], and **Shi Chen**[1,2]

[1]Department of Pediatrics, Indiana University School of Medicine, Indianapolis, IN 46202

[2]Herman B. Wells Center for Pediatric Research, Indiana University School of Medicine, Indianapolis, IN 46202

[3]Pathology and Laboratory Medicine, Indiana University School of Medicine, Indianapolis, IN 46202

[4]Department of Radiology and Imaging Sciences, Indiana University School of Medicine, Indianapolis, IN 46202

[5]Department of Anatomy and Cell Biology, Indiana University School of Medicine, Indianapolis, IN 46202

[6]Department of Microbiology and Immunology, Indiana University School of Medicine, Indianapolis, IN 46202

Abstract

Purpose—Plexiform neurofibromas (pNF) are pathognomonic nerve and soft tissue tumors of neurofibromatosis type I (NF1), which are highly resistant to conventional chemotherapy and associated with significant morbidity/mortality. Disruption of aberrant SCF/c-Kit signaling emanating from the pNF microenvironment induced the first ever objective therapeutic responses in a recent phase 2 trial. Sunitinib malate is a potent, highly selective RTK inhibitor with activity against c-Kit, PDGFR, and VEGFR, which have also been implicated in the pathogenesis of these lesions. Here, we evaluate the efficacy of sunitinib malate in a preclinical *Krox20;Nf1*$^{flox/-}$ pNF murine model.

Experimental Design—Proliferation, β-hexosaminidase release (degranulation), and Erk1/2 phosphorylation were assessed in sunitinib treated *Nf1*$^{+/-}$ mast cells and fibroblasts, respectively. *Krox20;Nf1*$^{flox/-}$ mice with established pNF were treated sunitinib or PBS-vehicle control for a duration of 12 weeks. pNF metabolic activity was monitored by serial [^{18}F]DG-PET/CT imaging.

Results—Sunitinib suppressed multiple *in vitro* gain-in-functions of *Nf1*$^{+/-}$ mast cells and fibroblasts and attenuated Erk1/2 phosphorylation. Sunitinib treated *Krox20;Nf1*$^{flox/-}$ mice

[*]**Correspondence should be addressed to**: Michael J. Ferguson, M.D., M.S., Assistant Professor, Indiana University School of Medicine, Children's Clinical Research Center, 705 Riley Hospital Drive, RI 2630, Indianapolis, IN 46202, Phone: (317) 278-3153, Fax: (317) 948-0616, micjferg@iu.edu.

Disclosure of Potential Conflicts of Interest

The authors have no competing financial interests.

exhibited significant reductions in pNF size, tumor number, and FDG uptake compared to control mice. Histopathology revealed reduced tumor cellularity and infiltrating mast cells, markedly diminished collagen deposition, and increased cellular apoptosis in sunitinib treated pNF.

Conclusions—Collectively, these results demonstrate the efficacy of sunitinib in reducing tumor burden in *Krox20;Nf1*$^{flox/-}$ mice. These preclinical findings demonstrate the utility of inhibiting multiple RTKs in pNF and provide insights into the design of future clinical trials.

Keywords

Sunitinib malate; Receptor tyrosine kinase; Neurofibromatosis type 1; Plexiform neurofibroma; Therapy; Preclinical mouse model

Introduction

Neurofibromatosis type I (NF1) is an autosomal dominant genetic disorder that affects approximately 1 in 3,500 individuals worldwide [1]. A hallmark feature of NF1 is the development of plexiform neurofibromas, which arise during early life from cranial and large proximal peripheral nerve sheaths. Plexiform neurofibromas have been found to affect 25-40% of children diagnosed with NF1 [2,3]. Although these tumors are considered benign, plexiform neurofibromas can cause severe disfigurement, disability, and even mortality from infiltration and compression of vital structures or from malignant transformation to malignant peripheral nerve sheath tumors (MPNSTs), which can occur in up to 10% of cases [4]. Surgical excision is the current standard of therapy for plexiform neurofibromas, however this can be technically challenging due to the vascularity and the infiltrative nature of these tumors resulting in a high rate of local recurrence as observed in two large institutional studies [5,6]. In many cases, the failure of standard therapeutic modalities have left patients, clinicians, and the research community searching for more effective treatment options.

The indolent growth characteristics of plexiform neurofibromas render them highly resistant to conventional cytotoxic chemotherapies. The potential for inducing malignant transformation to MPNSTs is another significant concern limiting the use of traditional DNA damaging agents in the treatment of these lesions. Thus, the development of targeted molecular therapies with the potential to induce growth arrest and/or regression of these slow-growing tumors represents a significant area of clinical morbidity.

NF1 is caused by germline mutations in the *NF1* tumor suppressor gene, which encodes the protein neurofibromin, a p21ras (Ras) guanine triphosphate (GTP)-activating protein (GAP) that regulates Ras activation states by accelerating the hydrolysis of active Ras-GTP to inactive Ras-GDP [7-12]. Ras-GTP recruits the serine-threonine kinase Raf-1 to the plasma membrane which then activates a series of downstream effectors such as Erk1/2 (p42/p44 MAPK) [13,14] that drive cell proliferation, differentiation, and survival in response to extracellular stimuli. Attempts to directly target Ras itself, however, have proven difficult, primarily due to its complex post-translational modification/activation. Given these limitations, it is necessary to test experimental therapeutics that inhibit RTKs that activate Ras in multiple cell types including Schwann cells in pNFs.

Sunitinib malate is an oral, small-molecule, multi-targeted receptor tyrosine kinase (RTK) inhibitor that was approved by the FDA for the treatment of renal cell carcinoma (RCC) and imatinib-resistant gastrointestinal stromal tumor (GIST). Sunitinib exhibits several key characteristics that make it an exceptional candidate for the treatment of NF1-related plexiform neurofibromas. Firstly, its biochemical properties include a reported IC50 for c-Kit between 1 and 10nM, which is a known RTK critical for pNF progression [15]. Secondly, sunitinib also inhibits two additional RTKs that are activated in multiple cell types within the pNF microenvironment, including: platelet-derived growth factor receptor (PDGFR) and vascular endothelial growth factor receptor (VEGFR) [16,17]. Targeting these two RTKs in other human cancers with similar molecular aberrations to pNF has shown some efficacy in both animal models and early human clinical trials [18,19]. Data from previous studies demonstrates that sunitinib inhibits PDGFR and VEGFR with IC50s in the nanomolar range [20]. Finally, the safety profile and pharmacokinetics of sunitinib are established in pediatric patients through a phase I clinical trial under the direction of the Children's Oncology Group [21].

In this study, we first demonstrated that sunitinib inhibits gain-in-functions within principle cellular constituents of the pNF microenvironment including *Nf1*$^{+/-}$ mast cells and fibroblasts, driven by hyperactive, Ras-dependent SCF and PDGF signaling. Further, we provide evidence that sunitinib malate induces growth arrest and regression of pNF in *Krox20;Nf1*$^{flox/-}$ mice validating broad inhibition of multiple RTKs as a potential therapy for NF1 patients with pNF.

Materials and Methods

Animals

The genetically engineered *Krox20;Nf1*$^{flox/-}$ mice have been previously described [22]. Animal care and experiments were conducted according to the guidelines established by the Indiana University Animal Care and Use Committee (IACUC). Progeny from these crosses were genotyped by polymerase chain reaction (PCR) as previously described [22].

In vivo experimental design and mouse data

Cohorts of age and sex-matched *Krox20;Nf1*$^{flox/-}$ mice were generated for drug treatment trials as described above. The metabolic activity of plexiform neurofibromas was assessed by fluorodeoxyglucose ([^{18}F] FDG) PET/CT imaging at baseline prior to treatment, 6 weeks, and 12 weeks of therapy as described in detail below. The experimental cohort consisted of 17 animals which were administered sunitinib malate 60 mg/kg/day by oral gavage. The placebo control group consisted of 9 mice that were administered the vehicle, phosphate buffered saline (PBS) by daily gavage. Treatment was initiated in 12- to 13-months of age. Daily weights were obtained with doses of drug and saline adjusted accordingly. Mice were treated for a duration of 12 weeks.

Dissection of Dorsal Root Ganglia and Measurement of Tumor Size

Immediately postmortem, mice were perfused and fixed in 4% paraformaldehyde. The dorsal root ganglia and peripheral nerves were dissected microscopically. Tumor volume

was derived by the formula approximating the volume for a spheroid = (0.52 × (width)^2 × length), as measured by calipers in the largest possible dimension according to our previously established methodology [23].

Histological Analysis

Paraffin sections were stained with hematoxylin and eosin (H&E), Masson trichrome, and toluidine blue to examine the tumor histomorphology as described previously [22]. Apoptosis was quantified histologically using TUNEL staining [24].

PET Imaging Analysis

Serial [^{18}F]DG-PET/CT imaging was employed to identify and profile the metabolic activity of plexiform neurofibromas at baseline and in response to treatment. CT images were used to place a standardized volume of interest (VOI) template over regions lateral to the spinal cord for quantification of FDG uptake. Registered and overlaid CT image data were subsequently used to map the course of the spinal cord in relation to specific anatomical landmarks identified within the vertebral column from the first lumbar (L1) to first sacral (S1) spinal levels. Three circular regions-of-interest (ROIs) were then placed at interpolated points corresponding to the spinal cord and bilateral dorsal root ganglia (DGRs). The circular ROIs then were combined to create VOIs for the spinal cord and bilateral DRGs. FDG images were acquired 45 min following injection of 0.5–1.0 mCi of FDG into the tail vein. Animals were anesthetized with isoflurane at 40 min post injection to immobilize prior to imaging [23].

Fibroblast and mast cell proliferation

Primary bone marrow derived mast cells and fibroblasts were cultured from *Nf1*$^{+/-}$ mice as previously described [25,26]. [^{3}H]Thymidine incorporation assays were performed to evaluate fibroblast and mast cell proliferation [27]. Briefly, cells were plated at a concentration of 4 × 10^3 cells/well in 96-well dishes in 200 mL of DMEM supplemented with 1% glutamine and 10% fetal calf serum (FCS), in a 37ºC, 5% CO_2 humidified incubator. Culture media was then switched to serum-free DMEM, and the cells were then cultured for 24–72 hrs. Tritiated thymidine ([^{3}H], PerkinElmer Life and Analytical Sciences, Boston, MA, USA) was added to cultures 6 hours prior to harvest on glass fiber filters (Packard Instrument Co.) and β-emission was measured.

β-Hexosaminidase Release Assay

Mast cell degranulation was evaluated by the β-hexosaminidase release assay [28]. In brief, bone marrow derived mast cells (BMMCs) were sensitized at 1 × 10^6/mL in the presence or absence of sunitinib in complete RPMI 1640 supplemented with 1.5 μg/ml anti-dinitrophenyl (DNP) IgE (clone SPE-7, Sigma-Aldrich) for 2 hours at 37°C in 5% CO_2. Cells were then washed once in Tyrode's buffer (130 mmol/L NaCl, 10 mmol/L HEPES, 1 mmol/L $MgCl_2$, 5 mmol/L KCl, 1.4 mmol/L $CaCl_2$, 5.6 mmol/L glucose, and 0.05% bovine serum albumin, pH 7.4) and resuspended at 2 × 10^6/mL in Tyrode's buffer. Cells were then stimulated with recombinant murine SCF (10 ng/mL, PeproTech) for 5 minutes at 37°C. After the cells were spun down, 30 μL of supernatant was transferred to a 96-well flat-

bottom plate. Then 30 μL of 1 mmol/L p-nitrophenyl-N-acetyl–D-glucosamide was added to each supernatant and mixed before incubation for 1 hour at 37°C. The reaction was terminated by the addition of 200 μL of 0.1 M Na_2CO_3-$NaHCO_3$ buffer, and optical density was read on a plate reader at a wavelength of 405 nm.

Western Blot Analysis

Western blot was performed to detect the phosphorylation of Erk1/2 following stimulation and sunitinib treatment [25,28].

Statistical Methods

Comparison of the mean tumor volume, differences in cellularity, and number of apoptotic cells between sunitinib-treated versus placebo-treated groups was performed using Student's t test or analysis of variance (ANOVA) with appropriate post-hoc correction. *P* values less than 0.05 were considered significant. Statistical analyses were performed with Prism 5.0 software (GraphPad, La Jolla, CA).

Results

Sunitinib inhibits multiple cellular functions, and biochemical activation of Erk1/2 in *Nf1*$^{+/-}$ fibroblasts and mast cells

We first tested whether sunitinib malate inhibits the proliferation of two key constituents of the pNF microenvironment, *Nf1* heterozygous mast cells and fibroblasts. Baseline [^{3}H]thymidine incorporation in unstimulated murine *Nf1*$^{+/-}$ fibroblasts was measured, followed by stimulation with PDGF (50 ng/mL) for 5 minutes in the presence of varying concentrations of sunitinib to generate a dose response curve (Figure 1A). At 100 nM of sunitinib, *Nf1*$^{+/-}$ fibroblast thymidine incorporation was reduced to basal levels, concordant with previously published results in NIH-3T3 cells [15]. We also observed similar results when we tested the ability of sunitinib to inhibit the proliferation of SCF-stimulated *Nf1*$^{+/-}$ mast cells (Figure 1B). We next examined the effects of sunitinib on *Nf1*$^{+/-}$ mast cell degranulation in response to SCF stimulation and found that sunitinib significantly reduced β-hexosaminidase release in a dose dependent fashion (p=0.02) (Figure 1C).

Sunitinib is a potent inhibitor of multiple RTKs including c-kit, VEGF, and PDGF. We tested the efficacy of sunitinib in inhibiting the biochemical activation of the Ras-MAPK signaling cascade, which drives gain-in-functions of multiple *NF1*(*Nf1*) haploinsufficient cell types. *Nf1*$^{+/-}$ fibroblasts were stimulated with PDGF (50 ng/mL) for 5 minutes in the presence or absence of sunitinib (100 nM). SCF and PDGF stimulation induced a robust increase in Erk1/2 phosphorylation in *Nf1*$^{+/-}$ mast cells (Figure 1D) and fibroblasts (Figure 1E), respectively which was markedly attenuated in sunitinib treated cells despite growth factor stimulation.

Reduced plexiform neurofibroma number and residual tumor size in *Krox20;Nf1*$^{flox/-}$ mice treated with sunitinib

Age and sex matched *Krox20;Nf1*$^{flox/-}$ mice (n=17) were treated with sunitinib malate at a dose of 60 mg/kg by daily oral gavage or a placebo control vehicle (n=9) as outlined in study

schematic presented in Figure 2A. Mice tolerated treatment well with no apparent adverse effects. Both vehicle control and sunitinib treated mice exhibited weight loss during the first two weeks of treatment, likely due to physiologic effects of the daily oral gavages. Body weight was maintained thereafter within 10% of baseline through the remaining ten weeks of therapy, with no significant difference between the experimental and control cohorts. After 12 weeks of sunitinib therapy, mice were sacrificed to evaluate the extent of residual tumor burden. Dorsal root ganglia at each spinal level were dissected microscopically and the identification of all suspected plexiform neurofibromas was confirmed by histological analysis. We observed a significant reduction in the mean number of plexiform neurofibromas per animal in sunitinib-treated *Krox20;Nf1*$^{flox/-}$ mice, with the sunitinib treatment group averaging 2.92 ± 0.51 tumors per mouse compared with 4.83 ± 0.72 tumors in the vehicle control treated cohort ($p<0.05$) (Figure 2B). Furthermore, mean tumor volume was reduced by 56% in the sunitinib treated mice as compared to the vehicle treated cohort over the same duration of therapy ($p< 0.05$) (Figure 2C).

Sunitinib therapy alters the plexiform neurofibroma microenvironment

Infiltrating *Nf1*$^{+/-}$ mast cells and fibroblasts are abundant within the plexiform neurofibroma microenvironment and play a critical role in promoting tumor growth and progression [16,17,29]. Therefore, we tested whether sunitinib treatment altered the cellular microarchitecture of these tumors *in vivo*. Following 12 weeks of therapy, histological sectioning of dorsal root ganglia (DRG) and peripheral spinal nerves were compared between the treatment and placebo groups. H&E stained cross-sections from DRG and peripheral spinal nerves of *Krox20;Nf1*$^{flox/-}$ mice treated with sunitinib demonstrate a marked decrease in tumor size, cellularity, and microarchitecture in representative plexiform neurofibromas compared to animals treated with the vehicle control (Figure 3A, top panel). Notably, Masson's Trichrome staining for collagen was diffuse and strongly positive throughout pNFs from the vehicle control cohort, while nearly absent in the sunitinib treated plexiforms (Figure 3A, middle panel). Mast cells, though abundant within the PBS treated plexiforms (Figure 3A, bottom panel), were dramatically reduced in number per high-power field (HPF) when enumerated in toluidine blue stained slides (Figure 3B, $p<0.05$). Finally, as shown in Figures 3C & D, there was a 4-fold increase in the number of apoptotic cells observed in the sunitinib treated group ($p<0.01$) compared to controls. Collectively, these observations provide evidence that sunitinib alters both the tumor size and cellular architecture of the tumor microenvironment in mice with pNF

Sunitinib treatment inhibits plexiform neurofibroma metabolic activity

In parallel experiments, small animal PET/CT imaging studies were performed to evaluate for changes in FDG uptake, which we have previously established as a biomarker of response to experimental therapy with imatinib in the *Krox20;Nf1*$^{flox/-}$ GEMM [23]. Serial FDG-PET/CT imaging studies were performed at baseline prior to the initiation of therapy, and prior to euthanasia at the end of the study. All image data sets were transformed to standardized uptake value units (SUVs) and all voxel values above a threshold of SUV=1.0 within a three dimensional volume of interest along the spine were integrated to form an FDG biomarker index. As expected, placebo treated mice showed a marked increase in the FDG uptake both at baseline and the conclusion of the study. By contrast, sunitinib treated

animals demonstrated a significant reduction in SUV uptake within the spinal cord and dorsal root ganglia at the end of the study (Figure 4A and B). Specifically, the SUV integral was reduced by nearly 70% in mice treated with sunitinib for 12 weeks of sunitinib therapy (p=0.03), compared to vehicle control mice which showed stable to mildly increased SUV integrals upon completion of the treatment course.

Discussion

Plexiform neurofibromas are complex nerve and soft tissue tumors which are pathognomonic of NF1, highly resistant to conventional chemotherapy, and associated with significant morbidity and mortality. To date, many promising therapies have failed to demonstrate efficacy in clinical trials [30-33], underscoring the importance of developing preclinical models which accurately recapitulate the biological complexity and growth kinetics of these neoplasms. *Krox20;Nf1*$^{flox/-}$ mice develop diffuse enlargement of peripheral nerve roots along the dorsal spinal column closely reminiscent of human plexiform neurofibroma tissue both morphologically and histopathologically, which provides a preclinical animal model to test experimental therapeutics [23].

Among the principle constituents of the plexiform neurofibroma microenvironment are infiltrating *Nf1*$^{+/-}$ mast cells and fibroblasts which are abundant within these tumors [29]. Mast cells are hematopoietic derived immune effector cells which are recruited to the microenvironment by aberrant SCF/c-Kit signaling and release a number of deleterious inflammatory mediators and trophic factors which potentiate pNF growth and progression [17]. *Nf1*$^{+/-}$ fibroblasts, stimulated by a number of growth factors including PDGF, deposit collagen comprising greater than 50 percent of the tumor dry weight [34]. The role of *Nf1*$^{+/-}$ vascular smooth muscle and endothelial cells to pNF initiation and progression is an understudied area of NF1 biology. Vascular smooth cell function is primarily controlled by PDGF receptor activation [35] and endothelial cell contribution to tumor neoangiogenesis is driven primarily by VEGF stimulation [36]. Previous studies demonstrate that both of these signaling axis are altered in both *Nf1*$^{+/-}$ vascular smooth muscle cells [37] and in endothelial cells [38]. Finally, *Nf1*$^{-/-}$ Schwann cells express many of these RTKs and secrete pathological concentrations of their respective ligands [39-43] which in part control multiple cell functions within the pNF.

Given the complexity of the tumor microenvironment in pNF, targeting multiple RTKs may be necessary in treating pNFs which is an emerging paradigm in tumor biology. Specifically, kinome analysis of both human and animals with different tumors suggest that inhibiting a single RTK can lead to activation of alternative signaling pathways that continue to drive tumorigenesis [44-48]. Furthermore, not all drugs inhibit the same target, such as c-kit, equivalently. Collectively, these observations provide rationale for testing a drug that inhibits multiple RTKs that are activated in pNF.

In comparison to imatinib mesylate which was used in a phase 2 clinical trial that resulted in tumor shrinkage in a subset of patients [49], sunitinib possesses greater biochemical inhibition of c-kit activity [15], a broader RTK profile [20] predicted to inhibit vascular smooth muscle, endothelium, and fibroblast function as well as established early phase

safety data in pediatric patients [21]. Based on this rationale, we formally tested whether sunitinib would inhibit or reduce pNF progression in a previously established, genetically engineered murine model.

Following 12 weeks of treatment, we observed a significant reduction in plexiform neurofibroma tumor burden (number and size) and metabolic activity as compared to vehicle treated controls. Historically, pNFs are slow growing tumors, even in our murine model, and response at 12 weeks has correlated well with tumor response clinically [23,49]. Upon completion of the study, postmortem histological analysis demonstrated a marked decrease in infiltrating $Nf1^{+/-}$ mast cells (by more than 50 percent) as well as dramatic reduction in fibroblast collagen deposition within the tumor microenvironment following sunitinib treatment. Additionally, TUNEL staining revealed an increase in apoptotic cells in sunitinib treated plexiform neurofibromas. These observations suggest that the biological effects of sunitinib treatment may relate not only to its ability to inhibit the recruitment and deranged functioning of *Nf1* haploinsufficient mast cells and fibroblasts within the tumor microenvironment, but also to trigger programmed cell death within the tumors themselves.

FDG-PET was utilized as a biomarker in these studies. Though FDG-PET is not sufficiently sensitive in the human system to detect therapeutic effects of drugs on plexiform neurofibromas, we found that attenuation in FDG uptake on PET imaging correlated with biological response (tumor shrinkage, decreased proliferative index, etc.) to both imatinib [23] and sunitinib treatment in the preclinical pNF murine model. Three dimensional, volumetric MRI is the modality currently used in clinical protocols for experimental therapeutics. The challenge with volumetric MRI is that it is a static measure of tumor response. Though FDG-PET imaging is useful only as a preclinical tool for pNF, the development of novel PET tracers that can be utilized as a sensitive biomarker in patients is an area of great need moving forward.

The results of this study are further supported by recently published data involving a number of other complementary pharmacologic approaches. While not directly comparable due to different study designs, sunitinib demonstrated a similar reduction in tumor progression in mice as imatinib even though each drug targeted different RTKs. To test whether administering drugs which target different RTKs in combination will reduce tumors better than a single agent will require further detailed studies. These studies are currently underway given the potential therapeutic benefit.

In addition, several additional RTKs inhibitors have also been demonstrated to promote tumor regression in other spontaneous and xenograft derived pNF models. Sorafenib is a multi-RTK inhibitor with activity against c-Kit, PDGFR, and VEGFR although significantly less potent than sunitinib with respect to c-kit inhibition (IC_{50} 68 nM vs 10 nM for sunitinib). In the spontaneous $Nf1^{flox/flox}$;*DhhCre* pNF murine model, sorafenib resulted in a modest reduction in tumor burden after eight weeks of treatment [50]. In contrast to the *Krox20*;$Nf1^{flox/-}$ model, $Nf1^{flox/flox}$;*DhhCre* mice exhibit robust biallelic inactivation of *Nf1* in primitive glial precursor cells during early embryogenesis (~E12.5) with a recombination efficiency on the order of 30-50% [51]. The early and more widespread *Nf1* recombination in the *DhhCre* model results in the development of diffuse, rapidly growing pNFs, thereby

circumventing the requirement for an *Nf1* haploinsufficient microenvironment in the genesis of these tumors which exists physiologically in human NF1 patients. Xenograft tumor models in athymic nude mice provide another preclinical context to evaluate the efficacy of candidate compounds, although the absence of a competent immune system limits their role in evaluating contributions of infiltrating mast cells and other inflammatory components of the pNF microenvironment which are known to play pivotal roles in tumor initiation and progression [17,23]. Nonetheless, nilotinib, a tyrosine kinase inhibitor with activity towards Bcr-abl, DDR, PDGFR, and c-kit receptor kinases, also demonstrated tumor shrinkage in such a model [52]. Although the biological responses achieved in these studies are difficult to directly compare, evidence of reduced tumor burden in multiple preclinical models achieved by targeting a similar spectrum of RTKs provides strong impetus for advancement of these pharmacotherapies toward early phase clinical studies.

Aside from RTK inhibition, pharmacologic MEK inhibitors including PD0325901 and AZ6244 have also demonstrated promising results in preclinical [53] and early phase clinical studies (unpublished data). Taken together, these observations provide impetus for the rational design of combinatorial strategies simultaneously interfering with paracrine growth signals emanating from the pNF microenvironment while also targeting aberrant Raf/MEK/ERK pathway activation in tumorigenic Schwann cells. Advantages of such an approach might include opportunities to minimize adverse side effects by lowering the respective doses of each agent and the potential to overcome drug resistance mechanisms mediated through adaptive reprogramming of the kinome [44-48].

In summary, preclinical testing of sunitinib in the *Krox20;Nf1*$^{flox/-}$ GEMM demonstrated reduction in plexiform neurofibroma number and size, decreased mast cell infiltration, diminished fibroblast collagen deposition, and reduced metabolic activity (FDG PET uptake) of these tumors. This study provides important experimental insights for the design of clinical trials that target multiple RTKs that are active in pNFs and underscores the need to understand the contribution of distinct biochemical pathways to tumor progression and initiation.

Acknowledgements

We thank Heather Daniel for administrative support.

Grant Support

This work was supported by the following grants: NIH R01 CA74177-15 (DWC), U01 NS055849-04 (DWC), P50 NS052606-10 (DWC), U54 CA196519-01 (DWC), Department of Defense (DOD) NF043032 (FCY), and NF073112 (FCY).

Abbreviations

NF1	Neurofibromatosis type 1
pNF	Plexiform neurofibroma
RTK	Receptor tyrosine kinase
PDGF	Platelet-derived growth factor

PDGFR	Platelet-derived growth factor receptor
VEGF	Vascular endothelial growth factor
VEGF	Vascular endothelial growth factor receptor
SCF	Stem cell factor
FDG	Fluorodeoxyglucose
PET	Positron emission tomography
CT	Computed tomography

References

1. Friedman, JM.; Riccardi, VM. Neurofibromatosis : phenotype, natural history, and pathogenesis. Vol. xiv. Johns Hopkins University Press; Baltimore: 1999. p. 381
2. Darrigo LG Jr, Geller M, Bonalumi Filho A, Azulay DR. Prevalence of plexiform neurofibroma in children and adolescents with type I neurofibromatosis. J Pediatr (Rio J). 2007; 83(6):571–573. [PubMed: 18046492]
3. Huson SM, Harper PS, Compston DA. Von Recklinghausen neurofibromatosis. A clinical and population study in south-east Wales. Brain. 1988; 111:1355–1381. Pt 6. [PubMed: 3145091]
4. Evans DG, Baser ME, McGaughran J, Sharif S, Howard E, Moran A. Malignant peripheral nerve sheath tumours in neurofibromatosis 1. J Med Genet. 2002; 39(5):311–314. [PubMed: 12011145]
5. Needle MN, Cnaan A, Dattilo J, Chatten J, Phillips PC, Shochat S, Sutton LN, Vaughan SN, Zackai EH, Zhao H, Molloy PT. Prognostic signs in the surgical management of plexiform neurofibroma: the Children's Hospital of Philadelphia experience, 1974-1994. J Pediatr. 1997; 131(5):678–682. [PubMed: 9403645]
6. Prada CE, Rangwala FA, Martin LJ, Lovell AM, Saal HM, Schorry EK, Hopkin RJ. Pediatric plexiform neurofibromas: impact on morbidity and mortality in neurofibromatosis type 1. J Pediatr. 2012; 160(3):461–467. [PubMed: 21996156]
7. Bourne HR, Sanders DA, McCormick F. The GTPase superfamily: a conserved switch for diverse cell functions. Nature. 1990; 348(6297):125–132. [PubMed: 2122258]
8. DeClue JE, Papageorge AG, Fletcher JA, Diehl SR, Ratner N, Vass WC, Lowy DR. Abnormal regulation of mammalian p21ras contributes to malignant tumor growth in von Recklinghausen (type 1) neurofibromatosis. Cell. 1992; 69(2):265–273. [PubMed: 1568246]
9. Gutmann DH, Boguski M, Marchuk D, Wigler M, Collins FS, Ballester R. Analysis of the neurofibromatosis type 1 (NF1) GAP-related domain by site-directed mutagenesis. Oncogene. 1993; 8(3):761–769. [PubMed: 8437860]
10. Hall A. Signal transduction through small GTPases--a tale of two GAPs. Cell. 1992; 69(3):389–391. [PubMed: 1316238]
11. Martin GA, Viskochil D, Bollag G, McCabe PC, Crosier WJ, Haubruck H, Conroy L, Clark R, O'Connell P, Cawthon RM, et al. The GAP-related domain of the neurofibromatosis type 1 gene product interacts with ras p21. Cell. 1990; 63(4):843–849. [PubMed: 2121370]
12. Wallace MR, Marchuk DA, Andersen LB, Letcher R, Odeh HM, Saulino AM, Fountain JW, Brereton A, Nicholson J, Mitchell AL, et al. Type 1 neurofibromatosis gene: identification of a large transcript disrupted in three NF1 patients. Science. 1990; 249(4965):181–186. [PubMed: 2134734]
13. Leevers SJ, Paterson HF, Marshall CJ. Requirement for Ras in Raf activation is overcome by targeting Raf to the plasma membrane. Nature. 1994; 369(6479):411–414. [PubMed: 8196769]
14. Stokoe D, Macdonald SG, Cadwallader K, Symons M, Hancock JF. Activation of Raf as a result of recruitment to the plasma membrane. Science. 1994; 264(5164):1463–1467. [PubMed: 7811320]

15. Abrams TJ, Lee LB, Murray LJ, Pryer NK, Cherrington JM. SU11248 inhibits KIT and platelet-derived growth factor receptor beta in preclinical models of human small cell lung cancer. Mol Cancer Ther. 2003; 2(5):471–478. [PubMed: 12748309]
16. Staser K, Yang FC, Clapp DW. Pathogenesis of plexiform neurofibroma: tumor-stromal/hematopoietic interactions in tumor progression. Annu Rev Pathol. 2012; 7:469–495. [PubMed: 22077553]
17. Staser K, Yang FC, Clapp DW. Mast cells and the neurofibroma microenvironment. Blood. 2010; 116(2):157–164. [PubMed: 20233971]
18. Heldin CH. Targeting the PDGF signaling pathway in tumor treatment. Cell Commun Signal. 2013; 11:97. [PubMed: 24359404]
19. Jain RK. Antiangiogenesis strategies revisited: from starving tumors to alleviating hypoxia. Cancer Cell. 2014; 26(5):605–622. [PubMed: 25517747]
20. Roskoski R Jr. Sunitinib: a VEGF and PDGF receptor protein kinase and angiogenesis inhibitor. Biochem Biophys Res Commun. 2007; 356(2):323–328. [PubMed: 17367763]
21. Dubois SG, Shusterman S, Ingle AM, Ahern CH, Reid JM, Wu B, Baruchel S, Glade-Bender J, Ivy P, Grier HE, Adamson PC, Blaney SM. Phase I and pharmacokinetic study of sunitinib in pediatric patients with refractory solid tumors: a children's oncology group study. Clin Cancer Res. 2011; 17(15):5113–5122. [PubMed: 21690570]
22. Zhu Y, Ghosh P, Charnay P, Burns DK, Parada LF. Neurofibromas in NF1: Schwann cell origin and role of tumor environment. Science. 2002; 296(5569):920–922. [PubMed: 11988578]
23. Yang FC, Ingram DA, Chen S, Zhu Y, Yuan J, Li X, Yang X, Knowles S, Horn W, Li Y, Zhang S, Yang Y, Vakili ST, Yu M, Burns D, Robertson K, Hutchins G, Parada LF, Clapp DW. Nf1-dependent tumors require a microenvironment containing Nf1+/−- and c-kit-dependent bone marrow. Cell. 2008; 135(3):437–448. [PubMed: 18984156]
24. Hiatt K, Ingram DA, Huddleston H, Spandau DF, Kapur R, Clapp DW. Loss of the nf1 tumor suppressor gene decreases fas antigen expression in myeloid cells. The American journal of pathology. 2004; 164(4):1471–1479. [PubMed: 15039234]
25. Ingram DA, Yang FC, Travers JB, Wenning MJ, Hiatt K, New S, Hood A, Shannon K, Williams DA, Clapp DW. Genetic and biochemical evidence that haploinsufficiency of the Nf1 tumor suppressor gene modulates melanocyte and mast cell fates in vivo. The Journal of experimental medicine. 2000; 191(1):181–188. [PubMed: 10620616]
26. Yang FC, Chen S, Clegg T, Li X, Morgan T, Estwick SA, Yuan J, Khalaf W, Burgin S, Travers J, Parada LF, Ingram DA, Clapp DW. Nf1+/− mast cells induce neurofibroma like phenotypes through secreted TGF-beta signaling. Hum Mol Genet. 2006; 15(16):2421–2437. [PubMed: 16835260]
27. Garbuzenko E, Nagler A, Pickholtz D, Gillery P, Reich R, Maquart FX, Levi-Schaffer F. Human mast cells stimulate fibroblast proliferation, collagen synthesis and lattice contraction: a direct role for mast cells in skin fibrosis. Clin Exp Allergy. 2002; 32(2):237–246. [PubMed: 11929488]
28. Khalaf WF, Yang FC, Chen S, White H, Bessler W, Ingram DA, Clapp DW. K-ras is critical for modulating multiple c-kit-mediated cellular functions in wild-type and Nf1+/− mast cells. J Immunol. 2007; 178(4):2527–2534. [PubMed: 17277161]
29. Staser K, Yang FC, Clapp DW. Plexiform neurofibroma genesis: questions of Nf1 gene dose and hyperactive mast cells. Curr Opin Hematol. 2010; 17(4):287–293. [PubMed: 20571392]
30. Babovic-Vuksanovic D, Ballman K, Michels V, McGrann P, Lindor N, King B, Camp J, Micic V, Babovic N, Carrero X, Spinner R, O'Neill B. Phase II trial of pirfenidone in adults with neurofibromatosis type 1. Neurology. 2006; 67(10):1860–1862. [PubMed: 17035676]
31. Gupta A, Cohen BH, Ruggieri P, Packer RJ, Phillips PC. Phase I study of thalidomide for the treatment of plexiform neurofibroma in neurofibromatosis 1. Neurology. 2003; 60(1):130–132. [PubMed: 12525736]
32. Widemann BC, Dombi E, Gillespie A, Wolters PL, Belasco J, Goldman S, Korf BR, Solomon J, Martin S, Salzer W, Fox E, Patronas N, Kieran MW, Perentesis JP, Reddy A, Wright JJ, Kim A, Steinberg SM, Balis FM. Phase 2 randomized, flexible crossover, double-blinded, placebo-controlled trial of the farnesyltransferase inhibitor tipifarnib in children and young adults with

neurofibromatosis type 1 and progressive plexiform neurofibromas. Neuro Oncol. 2014; 16(5): 707–718. [PubMed: 24500418]

33. Widemann BC, Salzer WL, Arceci RJ, Blaney SM, Fox E, End D, Gillespie A, Whitcomb P, Palumbo JS, Pitney A, Jayaprakash N, Zannikos P, Balis FM. Phase I trial and pharmacokinetic study of the farnesyltransferase inhibitor tipifarnib in children with refractory solid tumors or neurofibromatosis type I and plexiform neurofibromas. J Clin Oncol. 2006; 24(3):507–516. [PubMed: 16421428]
34. Jaakkola S, Peltonen J, Riccardi V, Chu ML, Uitto J. Type 1 neurofibromatosis: selective expression of extracellular matrix genes by Schwann cells, perineurial cells, and fibroblasts in mixed cultures. J Clin Invest. 1989; 84(1):253–261. [PubMed: 2500456]
35. Kraemer R, Nguyen H, March KL, Hempstead B. NGF activates similar intracellular signaling pathways in vascular smooth muscle cells as PDGF-BB but elicits different biological responses. Arteriosclerosis, thrombosis, and vascular biology. 1999; 19(4):1041–1050.
36. Ferrara N. VEGF and the quest for tumour angiogenesis factors. Nature reviews Cancer. 2002; 2(10):795–803. [PubMed: 12360282]
37. Li F, Munchhof AM, White HA, Mead LE, Krier TR, Fenoglio A, Chen S, Wu X, Cai S, Yang FC, Ingram DA. Neurofibromin is a novel regulator of RAS-induced signals in primary vascular smooth muscle cells. Hum Mol Genet. 2006; 15(11):1921–1930. [PubMed: 16644864]
38. Munchhof AM, Li F, White HA, Mead LE, Krier TR, Fenoglio A, Li X, Yuan J, Yang FC, Ingram DA. Neurofibroma-associated growth factors activate a distinct signaling network to alter the function of neurofibromin-deficient endothelial cells. Hum Mol Genet. 2006; 15(11):1858–1869. [PubMed: 16648142]
39. Mashour GA, Ratner N, Khan GA, Wang HL, Martuza RL, Kurtz A. The angiogenic factor midkine is aberrantly expressed in NF1-deficient Schwann cells and is a mitogen for neurofibroma-derived cells. Oncogene. 2001; 20(1):97–105. [PubMed: 11244508]
40. Hirota S, Nomura S, Asada H, Ito A, Morii E, Kitamura Y. Possible involvement of c-kit receptor and its ligand in increase of mast cells in neurofibroma tissues. Arch Pathol Lab Med. 1993; 117(10):996–999. [PubMed: 7692836]
41. Mashour GA, Driever PH, Hartmann M, Drissel SN, Zhang T, Scharf B, Felderhoff-Muser U, Sakuma S, Friedrich RE, Martuza RL, Mautner VF, Kurtz A. Circulating growth factor levels are associated with tumorigenesis in neurofibromatosis type 1. Clin Cancer Res. 2004; 10(17):5677–5683. [PubMed: 15355893]
42. Ryan JJ, Klein KA, Neuberger TJ, Leftwich JA, Westin EH, Kauma S, Fletcher JA, DeVries GH, Huff TF. Role for the stem cell factor/KIT complex in Schwann cell neoplasia and mast cell proliferation associated with neurofibromatosis. Journal of neuroscience research. 1994; 37(3): 415–432. [PubMed: 7513766]
43. Yang FC, Ingram DA, Chen S, Hingtgen CM, Ratner N, Monk KR, Clegg T, White H, Mead L, Wenning MJ, Williams DA, Kapur R, Atkinson SJ, Clapp DW. Neurofibromin-deficient Schwann cells secrete a potent migratory stimulus for Nf1+/− mast cells. J Clin Invest. 2003; 112(12):1851–1861. [PubMed: 14679180]
44. Duncan JS, Whittle MC, Nakamura K, Abell AN, Midland AA, Zawistowski JS, Johnson NL, Granger DA, Jordan NV, Darr DB, Usary J, Kuan PF, Smalley DM, Major B, He X, Hoadley KA, Zhou B, Sharpless NE, Perou CM, Kim WY, Gomez SM, Chen X, Jin J, Frye SV, Earp HS, Graves LM, Johnson GL. Dynamic reprogramming of the kinome in response to targeted MEK inhibition in triple- negative breast cancer. Cell. 2012; 149(2):307–321. [PubMed: 22500798]
45. Graves LM, Duncan JS, Whittle MC, Johnson GL. The dynamic nature of the kinome. Biochem J. 2013; 450(1):1–8. [PubMed: 23343193]
46. Johnson GL, Stuhlmiller TJ, Angus SP, Zawistowski JS, Graves LM. Molecular pathways: adaptive kinome reprogramming in response to targeted inhibition of the BRAF-MEK-ERK pathway in cancer. Clin Cancer Res. 2014; 20(10):2516–2522. [PubMed: 24664307]
47. Stuhlmiller TJ, Earp HS, Johnson GL. Adaptive reprogramming of the breast cancer kinome. Clin Pharmacol Ther. 2014; 95(4):413–415. [PubMed: 24413269]
48. Stuhlmiller TJ, Miller SM, Zawistowski JS, Nakamura K, Beltran AS, Duncan JS, Angus SP, Collins KA, Granger DA, Reuther RA, Graves LM, Gomez SM, Kuan PF, Parker JS, Chen X,

Sciaky N, Carey LA, Earp HS, Jin J, Johnson GL. Inhibition of Lapatinib-Induced Kinome Reprogramming in ERBB2-Positive Breast Cancer by Targeting BET Family Bromodomains. Cell Rep. 2015; 11(3):390–404. [PubMed: 25865888]

49. Robertson KA, Nalepa G, Yang FC, Bowers DC, Ho CY, Hutchins GD, Croop JM, Vik TA, Denne SC, Parada LF, Hingtgen CM, Walsh LE, Yu M, Pradhan KR, Edwards-Brown MK, Cohen MD, Fletcher JW, Travers JB, Staser KW, Lee MW, Sherman MR, Davis CJ, Miller LC, Ingram DA, Clapp DW. Imatinib mesylate for plexiform neurofibromas in patients with neurofibromatosis type 1: a phase 2 trial. Lancet Oncol. 2012; 13(12):1218–1224. [PubMed: 23099009]
50. Wu J, Dombi E, Jousma E, Scott Dunn R, Lindquist D, Schnell BM, Kim MO, Kim A, Widemann BC, Cripe TP, Ratner N. Preclincial testing of sorafenib and RAD001 in the Nf(flox/flox) ;DhhCre mouse model of plexiform neurofibroma using magnetic resonance imaging. Pediatr Blood Cancer. 2012; 58(2):173–180. [PubMed: 21319287]
51. Wu J, Williams JP, Rizvi TA, Kordich JJ, Witte D, Meijer D, Stemmer-Rachamimov AO, Cancelas JA, Ratner N. Plexiform and dermal neurofibromas and pigmentation are caused by Nf1 loss in desert hedgehog-expressing cells. Cancer Cell. 2008; 13(2):105–116. [PubMed: 18242511]
52. Wei J, Freytag M, Schober Y, Nockher WA, Mautner VF, Friedrich RE, Manley PW, Kluwe L, Kurtz A. Nilotinib is more potent than imatinib for treating plexiform neurofibroma in vitro and in vivo. PLoS One. 2014; 9(10):e107760. [PubMed: 25340526]
53. Jessen WJ, Miller SJ, Jousma E, Wu J, Rizvi TA, Brundage ME, Eaves D, Widemann B, Kim MO, Dombi E, Sabo J, Hardiman Dudley A, Niwa-Kawakita M, Page GP, Giovannini M, Aronow BJ, Cripe TP, Ratner N. MEK inhibition exhibits efficacy in human and mouse neurofibromatosis tumors. J Clin Invest. 2013; 123(1):340–347. [PubMed: 23221341]

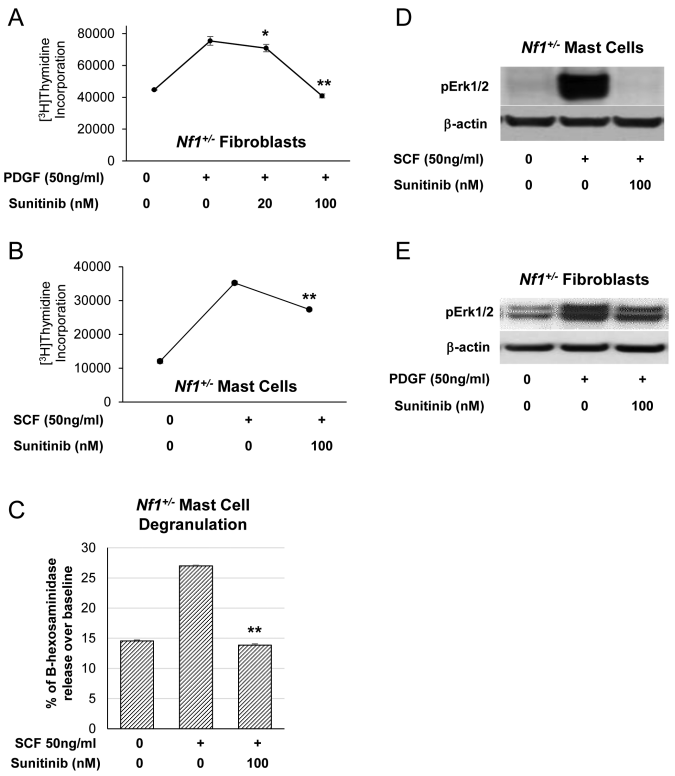

Figure 1. Sunitinib inhibits proliferation, functional activity, and Erk1/2 phosphorylation in *Nf1*$^{+/-}$ fibroblasts and mast cells

(A) *Nf1*$^{+/-}$ fibroblasts were stimulated with PDGF (50 ng/mL) for 5 minutes in the presence of increasing concentrations of sunitinib. [^{3}H]thymidine incorporation was measured as an indicator of fibroblast proliferation. A dose dependent response was observed with maximal inhibition of *Nf1*$^{+/-}$ fibroblast proliferative activity at sunitinib concentration of 100 nM. *P<0.05, **P<0.01 denotes statistical comparison between sunitinib treated fibroblasts vs those stimulated with PDGF alone. (**B**) *Nf1*$^{+/-}$ mast cells were then stimulated with SCF (50 ng/mL) for 5 minutes in the presence or absence of 100nM sunitinib. Proliferation was measured by ^{3}H]thymidine incorporation. **P<0.01 comparing mast cells treated with SCF plus sunitinib versus mast cells stimulated with SCF alone. (**C**) *Nf1*$^{+/-}$ mast cell degranulation stimulated by SCF (50 ng/mL) with or without sunitinib (100 nM) was quantified via a β-hexosaminidase release assay. **P<0.01 comparing sunitinib plus SCF treated mast cells to SCF stimulated mast cells alone. (**D**) Cultured *Nf1*$^{+/-}$ mast cells were stimulated with SCF (50ng/mL) for 5 minutes in the presence or absence of sunitinib (100 nM). Erk1/2 phosphorylation was detected by western blot with β-actin shown as a loading control. (**E**) *Nf1*$^{+/-}$ fibroblasts were stimulated with PDGF (50 ng/mL) for 5 minutes in the presence or absence of sunitinib (100 nM). Erk1/2 phosphorylation was detected by western blot with β-actin shown as a loading control.

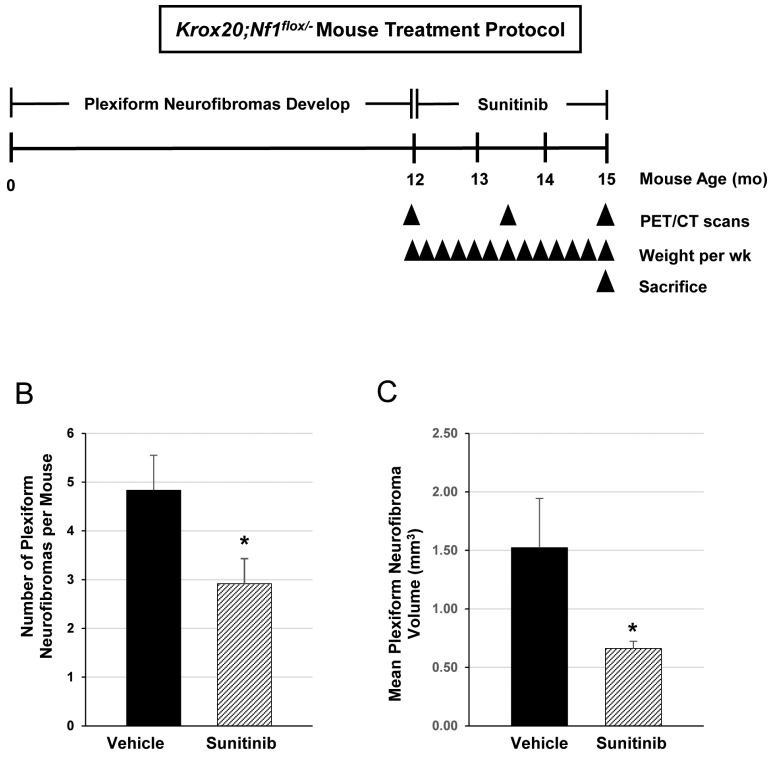

Figure 2. Sunitinib therapy reduces plexiform neurofibroma tumor burden *Krox20;Nf1*$^{flox/-}$ mice

(A) Cohorts of age and sex matched *Krox20;Nf1*$^{flox/-}$ mice were treated with either sunitinib or vehicle control (PBS) as outlined in the schematic. Treatment was initiated at a mean age of 12-13 months. Drug was administered by daily oral gavage for a duration of 12 weeks. Serial PET/CT scans were performed at baseline, 6 weeks, and 12 weeks of treatment in six mice from each cohort. Upon reaching the 12 week time point, mice were euthanized and tissues were dissected/harvested for histopathological analysis. **(B)** Mean number of tumors from *Krox20;Nf1*$^{flox/-}$ mice treated with vehicle versus sunitinib. *P< 0.05 comparing vehicle to sunitinib. **(C)** Mean volume of plexiform neurofibromas from peripheral nerves of *Krox20;Nf1*$^{flox/-}$ mice treated with vehicle versus sunitinib. *P< 0.01 comparing vehicle to sunitinib.

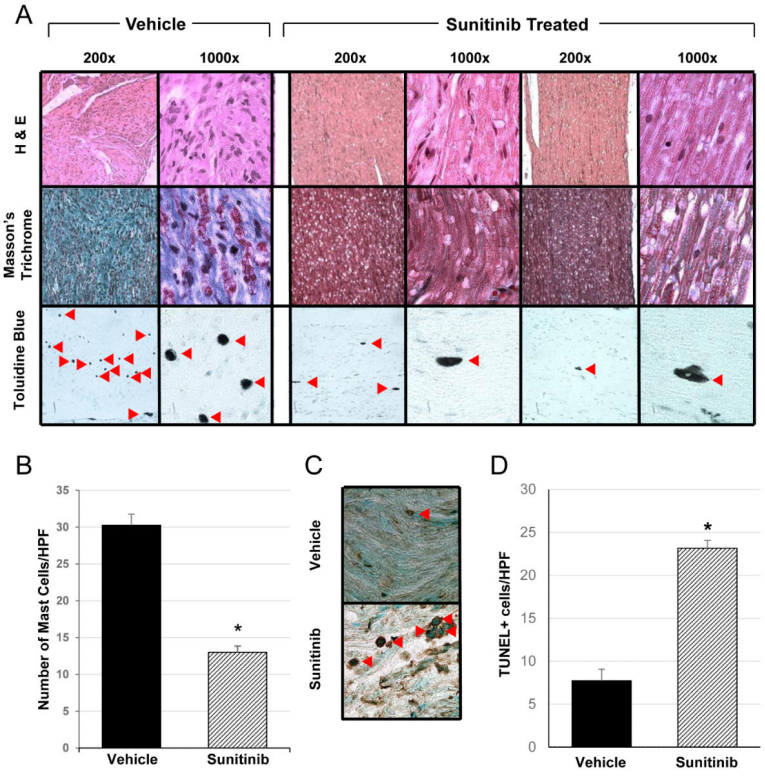

Figure 3. Histopathological characterization of plexiform neurofibromas in sunitinib treated *Krox20;Nf1*$^{flox/-}$ mice

(A) Histopathological analysis of the Krox20;Nf1flox/- mice following 12 weeks treatment with either sunitinib or vehicle. Representative H&E (top panel), Masson's Trichrome (middle panel), toluidine blue (bottom panel) stained pNF sections are shown for both vehicle and sunitinib treated mice (magnification 200x, 1000x). Sunitinib treated pNFs demonstrated reduced cellularity, markedly decreased collagen deposition, and reduced mast cell infiltration. Red arrowheads denoted toluidine blue stained mast cells within the pNF microenvironment. **(B)** The number of infiltrating mast cells per high power field (HPF) were counted in toluidine blue stained sections of tumors from *Krox20;Nf1*$^{flox/-}$ mice treated with sunitinib compared to the vehicle control (n=8 animals per group). *P<0.001 comparing sunitinib treated mice to the vehicle control. **(C)** Representative photomicrographs of immunohistochemical TUNEL staining performed on pNFs from vehicle vs sunitinib treated *Krox20;Nf1*$^{flox/-}$ mice (400x magnification). Red arrowheads denote apoptotic cells identified by TUNEL staining. **(D)** The number of TUNEL positive cells per HPF in pNFs from the sunitinib treated cohort versus the vehicle control were enumerated by manual counting. (n=7 animals per group). *P<0.001 denotes statistical comparison between sunitinib and the vehicle control groups.

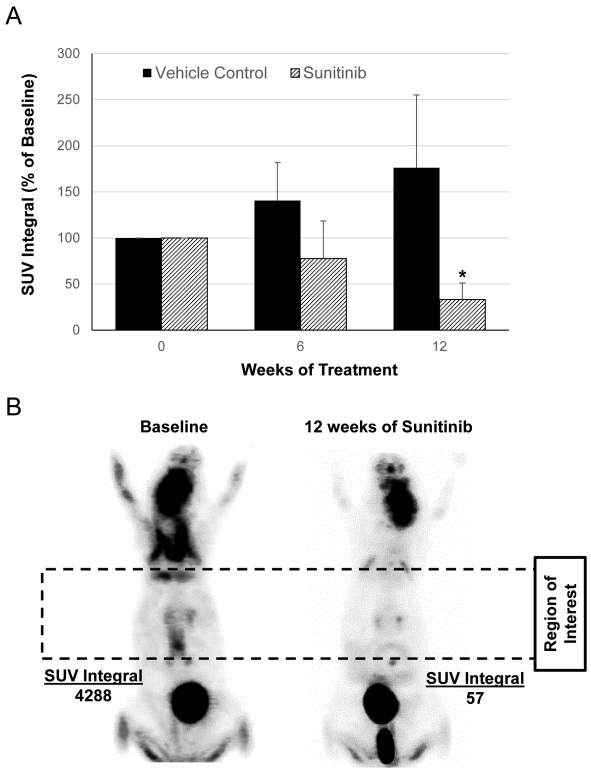

Figure 4. FDG-PET/CT imaging of plexiform neurofibroma metabolic activity in sunitinib and vehicle treated mice

(A) Tumor metabolic activity was assessed by serial PET/CT imaging of FGD uptake in sunitinib and vehicle treated *Krox20;Nf1*$^{flox/-}$ mice (n = 6 animals per group). The SUV integral represents a measure FDG retention within a 3D volume of interest including the spinal cord and bilateral spinal nerve roots. Blue bars represent the SUV integral at baseline prior to treatment, red bars after 6 weeks of treatment, and green bars at the 12 weeks endpoint. The SUV integral (as a percentage of baseline) was significantly reduced in the sunitinib treated mice as compared to the vehicle treated cohort after 12 weeks of treatment. *P<0.05 denotes statistical comparison between 12 weeks of sunitinib treatment versus baseline. **(B)** FDG-PET imaging in a representative sunitinib treated mouse at baseline and 12 week time points. The dotted box represents the SUV region of interest for assessing FDG uptake over the dorsal root ganglia and spinal column.